Technical Paper

ISSN 1997-1400 Int. J. Pavement Res. Technol. 8(5):305-314

Development of Rut Prediction Models from an Instrumented In-Service Test Section on Interstate-35

Nur Hossain[1+], Dharamveer Singh [2], and Musharraf Zaman [3]

Abstract: This paper presents development of two different field rut prediction models based on data collected from an instrumented pavement section on I-35 in McClain County, Oklahoma. Two rut prediction models, vertical strain-based (VSB) and shear strain-based (SSB), were developed utilizing four years of pavement and environmental data and from approximately 18.7-million accumulated axles. The VSB model considers vertical strain on the top of the aggregate base layer, while the SSB model was based on the shear strain in the Hot Mix Asphalt (HMA) layer. Falling Weight Deflectometer (FWD) tests were conducted over a wide range of temperature to establish modulus and temperature relationship. A pavement analysis software, WinJULEA, was used to develop correlations between temperature and vertical and shear strains for single and tandem axles. In addition, field rut measurements were conducted periodically using a straight edge-rut gauge combination and a Face Dipstick®. A systematic methodology to develop the rut prediction models is presented in the paper. The correlation coefficient (R^2) for the VSB and the SSB models were found to be 0.78 and 0.72, respectively. Statistical analyses showed that both models predicted rut with a similar level of accuracy. The results from this study are expected to be useful in predicting rut of state highway pavements under similar traffic and environmental conditions. In addition, data collected from this study may be used for local calibration of rut prediction model available in the Mechanistic-Empirical Pavement Design Guide (MEPDG).

DOI: 10.6135/ijprt.org.tw/2015.8(5).305
Key words: *Falling Weight Deflectometer; Field rut measurements; HMA; MEPDG; Rut; Rut prediction models; Strain-temperature correlations.*

Introduction

According to the Mechanistic-Empirical Pavement Design Guide (MEPDG) [1] the two most important failure criteria for flexible pavements are: (i) fatigue cracking at the bottom of Hot Mix Asphalt (HMA) layer and (ii) rutting along the wheelpaths on pavement. Rutting is a major concern for the integrity of pavement structures and traffic safety. Accurate prediction of rut for an in-service pavement under actual vehicular traffic loading and environmental conditions is critical for effective pavement design.

Several researchers have developed rut prediction models from laboratory data [2-4]. For example, Allen and Dean [2] proposed a model based on laboratory tests performed on asphalt mixes. However, the ruts predicted from their model were not compared with the actual ruts measured from in-service pavements. Similarly, Leahy [3] developed a model based on repeated load triaxial and creep tests performed in the laboratory. However, the implementation of the model was limited due to the complexity of model parameters. In a similar study, Williams et al. [4] used results from the WesTrack project to develop a correlation for predicting pavement rutting from accelerated rut tests (Asphalt Pavement Analyzer) in the laboratory. This model was developed mainly from laboratory test data and is limited to similar pavement and environmental conditions at WesTrack.

Recently, several studies have been conducted with a focus on developing rut prediction models from field data [5-9]. For example, Ali et al. [5] developed a model using vertical strain data collected from 61 Long Term Pavement Performance (LTPP) Test Sections. However, their study did not consider the contribution of shear strain in the development of the model. Similarly, Hand et al. [6] developed a model based on data from the accelerated pavement testing facility at WesTrack, located in Reno, Nevada. It was concluded that rutting was mainly controlled by shear deformation in the HMA layer, thus, vertical deformation in the pavement layers was neglected. Kim et al. [7] presented a model using data from 39 in-service flexible pavements in Michigan. Their model accounts for the distribution of rut in the subgrade, subbase, base, and HMA layers. Although the model predicts rut depth reasonably well, one of the disadvantages of the model is that it has many variables making it difficult to use. Although some variables in the model are dependent on each other, they did not provide any justifications for including all the variables in the model. Similarly, the model presented by Zhou et al. [8] is based on the data collected from the Accelerated Load Facility (ALF), located at Turner-Fairbank, VA, from 1993 through 2001. Three different models were developed to predict rut at primary, secondary, and tertiary stages. Although the model defined the three stages of permanent deformation fairly well, consideration of three stages made it complicated. Recently, Selvaraj [9] developed two different models based on the results obtained from accelerated pavement testing facility at the National Center for Asphalt Technology (NCAT) test track. One of the models was a vertical strain-based (VSB) model and the other was a shear strain-based (SSB) model. Although these models predicted

[1] Kleinfelder, Inc. 10835 East Independence, Suite 102, Tulsa, OK 74116, USA.
[2] Department of Civil Engineering, Indian Institute of Technology, Bombay, Powai, Mumbai, 400076, India.
[3] The University of Oklahoma, 201 Stephenson Pkwy, Suite 4200, Norman, OK 73019, USA.
[+] Corresponding Author: E-mail nhossain@kleinfelder.com
Note: Submitted February 13, 2015; Revised May 30, 2015; Accepted July 1, 2015.

pavement rut reasonably well, they did not consider any variations in traffic loading. The aforementioned studies indicate a need for rut prediction models based on the actual traffic and environmental data from an in-service pavement.

The present study was undertaken to develop two field rut prediction models from data collected along a 305-meter long instrumented Test Section in McClain County, Oklahoma. The thickness of the Test Section was purposely designed to be thin so that it would fail in a relatively short period of time, thus allowing its in-service performance to be monitored over its entire service life. This design resembles similar accelerated pavement testing (APT) concepts, but involves actual vehicular traffic and environmental conditions rather than controlled conditions generally used in APT. The pavement performance data, environmental data, and traffic data were collected at regular intervals. A series of falling weight deflectometer (FWD) tests and rut measurements were conducted to develop the rut prediction models.

Objectives

The objectives of this study were:

(1) To monitor pavement performance and measure rut progression in a Test Section using two different methods: (i) straight edge-rut gauge combination and (ii) Face Dipstick®,
(2) To conduct FWD tests having a wide range of temperatures on the Test Section, and establish HMA modulus and temperature relationship,
(3) To develop vertical strain-temperature and shear strain-temperature relationships for single and tandem axles using WinJULEA, and
(4) To develop vertical strain and shear strain based rut prediction models using actual vehicular traffic loading and environmental conditions.

Construction and Instrumentation of the Test Section

Test Section

Location of the Test Section

The instrumented Test Section used in this study is located in McClain County, Oklahoma, on the southbound (right) lane of Interstate-35. To record the traffic data, a weigh-in-motion (WIM) station was installed approximately 1,200-meter south of the Test Section. The Test Section and the WIM site start at approximately Mile Post 95 and ends at Mile Post 91.

Layout of the Test Section

The Test Section consists of five pavement layers. The top layer is 50-mm thick constructed with a HMA mix having 12.5-mm Nominal Maximum Aggregate Size (NMAS). The mix is prepared with a Performance Grade (PG) 64-22 asphalt binder. The second layer is 125-mm thick and is constructed with a HMA mix having a NMAS of19-mm. This layer incorporates a recycled mix involving a PG 64-22 binder and 25% reclaimed asphalt pavement (RAP). The third layer is a 200-mm thick aggregate base layer having Oklahoma Department of Transportation (ODOT) type "A" gradation. The fourth layer consists of a 200-mm thick subgrade layer stabilized with 12% Class C fly ash. The bottom layer is natural subgrade soil, consisting of lean clay with a liquid limit of 33 and a plasticity index of 15.

Instrumentation

Twelve asphalt strain gauges were installed to measure longitudinal and transverse strains at the bottom of the HMA layer. Also, one earth pressure cell was installed at the top of each pavement layer, namely natural subgrade layer, stabilized subgrade layer, and aggregate base layer to measure traffic-induced normal stresses. In addition, five temperature probes were installed to measure temperature variations in the HMA layer at selected depths (5-mm, 50-mm, 90-mm, 180-mm and 254-mm) from the pavement surface. Three lateral positioning sensors were also installed on the top of the HMA layer to determine vehicle wheel wander over the Test Section. A sketch of the Test Section is shown in Fig. 1.

Traffic

After finishing the construction and instrumentation of the Test Section, it was opened to traffic on May 30, 2008. Traffic and environmental data are being collected since then. The WIM site was instrumented with inductive loops and piezoelectric sensors to capture axle configuration, weight, distance between axles, and other pertinent data for each vehicle passing through the Test Section. These data, along with the field performance data were used in this study to develop rut models. Approximately four years of traffic data (i.e., from May 30, 2008 to May 2, 2012) were used to develop the rut prediction models. The test section was designed based on the following traffic assumption: AADT: 42,500; overloaded trucks: 16%, truck growth rate: 2%, design direction: 56%, and design life: 5 years.

Test Stations

A total of six stations (Stations 1 through 6) were selected for monitoring pavement performance at the Test Section. These stations were marked along the outside wheel path and were located at approximately 30.5-meter intervals. Only Station 3 was within the instrumentation array. Road straps were laid down on the pavement surface at all the stations during the first field test on August 21, 2008.

Field Test Facility and Data Collection

Various field performance data were collected from the Test Section to evaluate pavement response under actual vehicular traffic and environmental conditions. These activities included evaluation of layer moduli through FWD tests, permanent deformation (rut) evaluation through straight edge-rut gauge combination and Face Dipstick®, and pavement temperature data and traffic data through the WIM station. Since the Test Section was located on I-35, which has extremely high and heavy traffic volume, it was not practical to

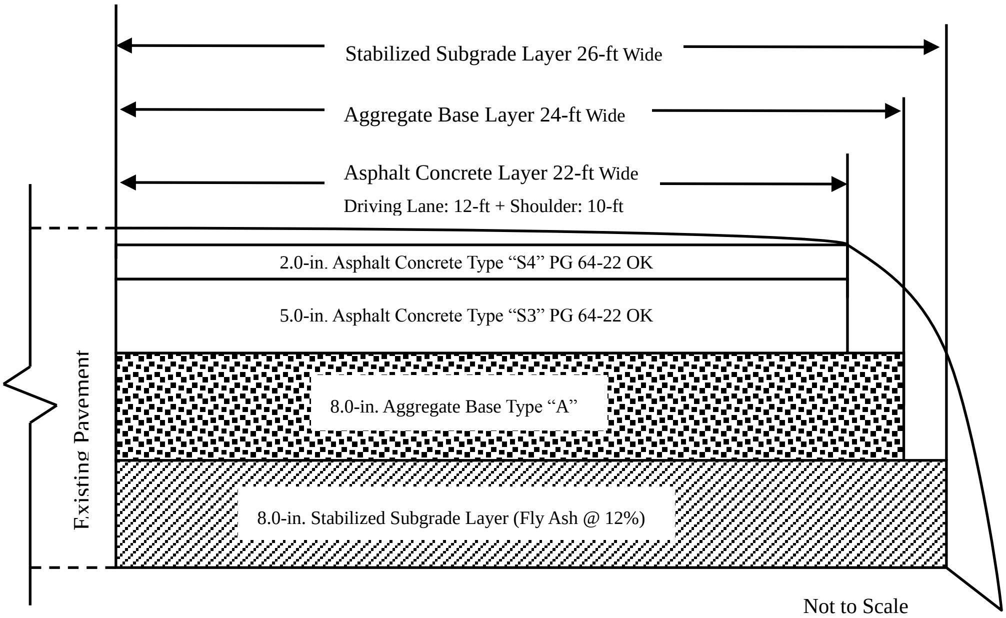

Fig. 1. Sketch of the Test Section.

close the lanes frequently to collect pavement performance data. Therefore, field performance tests were conducted once every three months.

FWD Data

In this study, pavement layer moduli back-calculated from the FWD data was used to develop the models. A Dynatest FWD (Model 8002-057) with seven velocity sensors located at 0-mm, 200-mm, 300-mm, 609-mm, 914-mm, 1,219-mm, and 1,828-mm from the center, as recommended by the ASTM D 4694 test method, was used to conduct the FWD tests. The loading pattern comprised of three seating drops plus one load drop from different heights. Four different loads levels (27-kN, 40-kN, 53-kN and 68-kN) were used for HMA layers, as recommended by the ASTM D4694 test method. The FWD tests were conducted on a wide range of pavement temperatures (from 10℃ to 43℃), and a correlation between HMA modulus and mid-depth pavement temperature was established as presented in Fig. 2 with starting field measurement on May 30, 2008. Before opening the Test Section to actual traffic, FWD data were collected at different times of the day from May 16, 2008 through May 20, 2008. Also, the FWD data were collected on August 21 and December 3, 2008, May 19 and October 28, 2009, and May 18, 2010, after lane closures in the morning. The FWD data were used to back-calculate the layer moduli, using MODULUS 6.0 software. As it can be seen that the modulus value decreases with an increase in temperature. The different modulus values at same temperature are observed because of aging of pavement. The E value of a pavement increases with time due to oxidative aging which results in stiffer binder. A detailed discussion on the back-calculation procedure can be found in Hossain [10]. The following modulus-temperature relationship was obtained for the HMA layers (Fig. 2):

$$E = 30713\, e^{-0.081\,T} \quad (R^2 = 0.86) \tag{1}$$

where,
E = Average modulus of HMA layers (MPa), and
T = Mid-depth pavement temperature (^{o}C).

Rut Measurements

Rut measurements were conducted along the transverse direction of traffic flow at six selected test stations (Stations 1 through 6). The rut measurements were taken along the road-straps laid on the test stations ensuring that the measurement locations did not change with time. Two significantly different methods, a straight edge-rut gauge combination and a Face Dipstick®, were used to measure rut in the field. During the first three field tests (on August 21, 2008, December 3, 2008 and January 8, 2009), the straight edge-rut gauge combination method was used. The rut data obtained from the straight edge-rut gauge combination exhibited some inconsistencies for two reasons: (i) since the straight edge was not long enough, it had to be shifted during measurements to cover the entire width of the Test Section, which changed the reference points; and (ii) the rut gauge, having an increment of 1.27-mm, was not sensitive enough to measure small changes in rut values. Consequently, a more sophisticated piece of equipment, Face Dipstick®, capable of measuring rut with 0.0254-mm accuracy, was used for measuring ruts from May 19, 2009 onward. Two different intervals, 150-mm and 300-mm (called moon-foot spacing), were used to measure rut with the Face Dipstick®. On May 19, 2009, the rut values were measured using both the straight edge-rut gauge combination and the Face Dipstick® for comparison. As expected, the Face Dipstick® provided much more consistent and accurate rut values than the straight edge-rut gauge combination.

Rut Progressions in the Test Section

According to Zhou et al. [8], flexible pavement rutting can be categorized into three distinct stages: primary, secondary, and

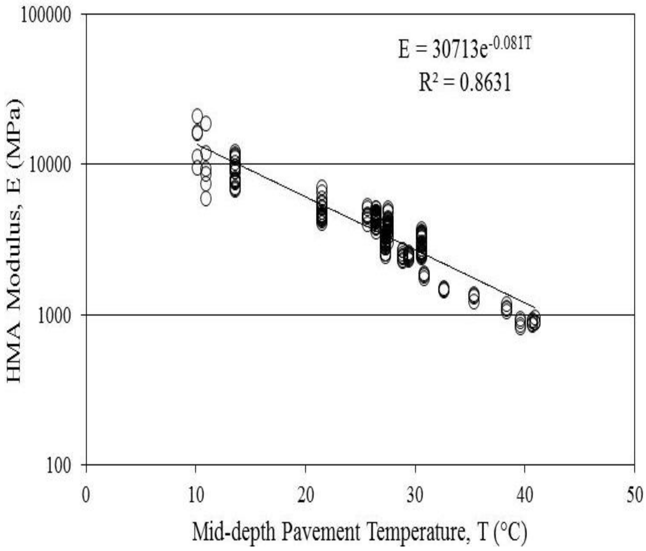

Fig. 2. HMA Modulus-Temperature Correlations.

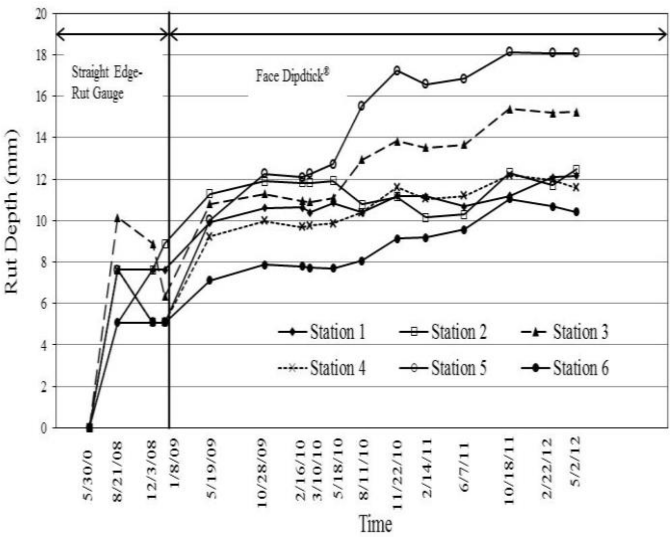

Fig. 3. Rut Progressions in the Test Section.

tertiary. The rutting progressions in all six test stations are presented in Fig. 3, with each curve representing the rutting progression at a specific station. As of May 2012, approximately four years after the Test Section was opened to traffic, both the primary and secondary stages were observed. The tertiary stage has not been observed yet. During the primary stage (from May 30, 2008 through August 21, 2008), the rutting rate was relatively high. After the primary stage, the rutting progression rate decreased and reached a nearly constant value at the secondary stage (from around September 2008 to May 2, 2012). A similar rut progression trend was observed in the AASHO road test [11-12] and in the NCAT test tracks [9], where the rutting rate decreased as the number of axles increased. It is evident from Fig. 3 that rut values decreased significantly when measured with traditional straight edge-rut gauge combination at some stations even with increased axle passes and time. These observations necessitated the inclusion of rut measurements with Face Dipstick®.

After roughly four years of service, the maximum rut of 18.14-mm and the minimum rut of 10.41-mm were observed at Station 5 and Station 6, respectively. The corresponding cumulative axles traversing the Test Section were about 18.7-million. Although the rut values increased with time, most of the rut was accumulated during the summer months. For example, out of 18.14-mm rut measured at Station 5, approximately 12.11-mm was accumulated during the summer months. Also, the rate of rutting during the first summer month was much higher than in the second, third, and fourth summer months, although the cumulative axles during each summer were similar (approximately 1.2-million). Similar behavior of accumulation of rut in summer has been reported in previous studies (e.g., AASHO road test, NCAT test track).

Development of Rut Prediction Models

Historically, two different approaches have been used to predict pavement rutting [9]. One approach involves predicting pavement rutting by calculating vertical strains on the top of the aggregate base or subgrade. Another approach is based on the consideration of shear strain calculation in the HMA layer. Although it is widely accepted that vertical strain on the top of the aggregate base layer or the subgrade layer can be a major contributor to pavement rutting [2, 12], recent studies have shown better correlations of shear strain along the tire edge to HMA rutting. For example, in a NCAT study Selvaraj [9] observed that the magnitude of shear strain was strongly correlated with rutting. Other researchers [7, 13] have also shown that it is difficult to control the pavement rutting only by controlling the vertical compressive strain on the top of the subgrade soil. Therefore, both vertical strain-based and shear strain-based approaches were explored in the present study to develop the rut prediction models.

Vertical Strain-based (VSB) Rut Prediction Model

Methodology

The methodology used here to develop the VSB model is presented in Fig. 4. A similar methodology was used by Selvaraj [9] for developing rut prediction models from the Test Sections at NCAT. One major difference between Selvaraj's methodology and the present methodology is the type of traffic loading. The NCAT test track is a closed facility and the traffic loading is achieved through a single truck's repeated loading over the track, whereas in the present study, response of an in-service pavement under actual vehicular traffic loading which involves different classes of trucks, variable weights, different axle configurations, tire pressure, etc. was monitored. The rut prediction models were developed by considering loads coming from FHWA Class 4 to FHWA Class 13 vehicles.

In the flow chart (Fig. 4), the time stamp (i) is used to link variables, namely measured mid-depth pavement temperature (T_i) and traffic axle count (N_i) for a particular time period. The calculated vertical strain on the top of the pavement layers at a particular time (ε_i) and number of axle passes at that time (N_i) were selected as the independent variables in the model. The total measured rut depth (Rut_i) at a particular time was calculated as a sum of the previous period's total rut (Rut_{i-1}) plus incremental rutting caused by additional traffic (N_i) at the calculated strain level (ε_i) for the current time increment.

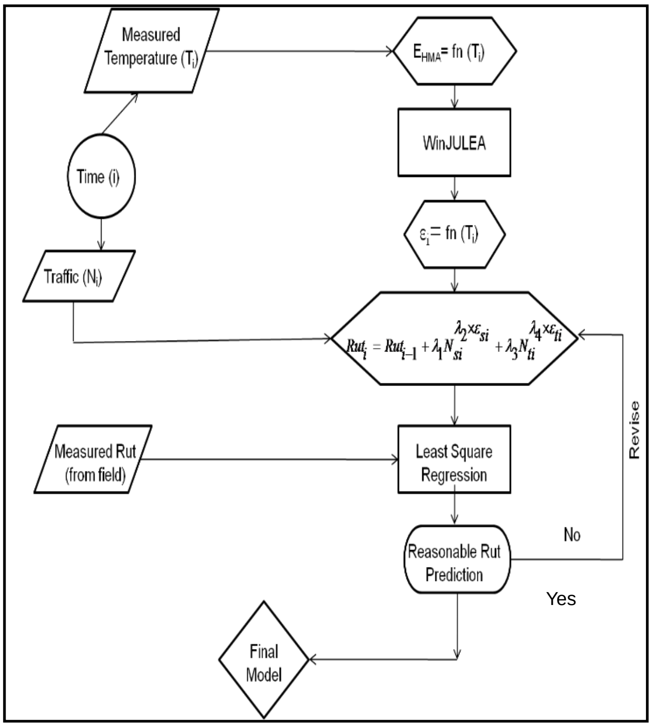

Fig. 4. Vertical Strain-based Rut Prediction Model Methodology Flow Chart.

The following data were used in developing the vertical strain-based rut model:

(1) Material properties data: Moduli of pavement layers, namely HMA layer, aggregate base layer, stabilized subgrade layer and natural subgrade layer, were back-calculated from the FWD data. The modulus of HMA layer was calculated using Eq. (1). The average moduli of the aggregate base layer, stabilized subgrade layer, and natural subgrade layer, obtained from the FWD test data, were found to be 194.4-MPa, 480.6-MPa and 138.6-MPa, respectively.

(2) Environmental data: Mid-depth pavement temperature data measured from installed temperature sensors was used. Pavement temperature was measured every minute but only hourly averages were stored.

(3) Traffic data: Traffic configuration such as axle type and weight, irrespective of vehicle class, was recorded from the WIM station.

(4) Pavement performance data: Rut data measured using straight edge-rut gauge combination and Face Dipstick® were used.

(5) Tire inflation pressure: A default hot tire inflation pressure of 827-kPa, as recommended in the MEPDG [1], was used in this study.

Vertical Strain Calculation on the Top of Aggregate Base

As noted earlier, measured vertical strain response on the top of pavement layers is an important element of the rut model. There was no strain gauge installed to measure the vertical strain on the top of aggregate base or subgrade layers. Therefore, WinJULEA was used to predict vertical strain on the top of the aggregate base and the natural subgrade layers due to vehicular traffic. WinJULEA is a commonly used multi-layered linear elastic analysis software, which is also incorporated in the MEPDG [1], for calculating pavement response. Also, previous studies (see e.g., Monismith [14]) showed that linear elastic analysis is a reasonable tool for rut evaluation when the pavement temperature does not exceed 40°C. Since the maximum pavement temperature (mid-depth) measured in the Test Section was below 47℃, it was considered reasonable to use the linear elastic model to predict vertical strains for developing the rut prediction model. WinJULEA analyses showed that, for a particular vehicular load, the maximum vertical strain is experienced on the top of the aggregate base layer. For example, in Fig. 5, a representative vertical strain distribution from WinJULEA analyses is shown for a particular temperature and a particular vehicle load. It is observed from Fig. 5 that the maximum strain observed on the top of aggregate base layer was 5.83x10-4 mm/mm, which is significantly higher than the strains in other layers of the pavement. Therefore, vertical strain on the top of the aggregate base layer was used to develop the VSB model.

Vertical Strain-Temperature Correlations

An important step in developing the VSB model was to develop correlations between vertical strain and mid-depth pavement temperature. The following steps were used to develop the vertical strain-temperature correlations:

Step-1: A mid-depth pavement temperature for a particular hour was selected. Then, the HMA modulus for that particular temperature was calculated using Eq. (1).

Step-2: Then, for that particular hour, vehicular traffic data were obtained from the WIM station. In WinJULEA calculations, steering axles and tandem axles were analysed separately because of differences in vertical strain distribution. A steering axle has single wheels at axle ends, while a tandem axle has dual wheels at axle ends. Primary strain calculation through WinJULEA showed that strain induced by one wheel does not contribute to (or interfere with) the strain induced by the other wheel, in the case of steering axles. However, in the case of tandem axles, WinJULEA calculations showed that strain induced by one wheel (of the dual wheel) overlaps with the strain contributed by the other wheel. Several vehicles including the lowest and the highest steering axle weights were selected and half steering axle weights noted (irrespective of class). Vertical strains were calculated for each axle weight using WinJULEA and were used to obtain a correlation between vertical strain and half steering axle weights at that particular temperature. The general form of the correlation between vertical strain and half steering axle weights can be expressed by Eq. (2):

$$\varepsilon_s = C_1(half\ steering\ axle\ weight) + C_2 \tag{2}$$

where,

ε_s = Vertical strain from steering axle, and

C_1, C_2 = Variable regression constants.

Similarly, a linear correlation was developed for vertical strain and 1/4th tandem axle weights for that particular temperature, as given by Eq. (3):

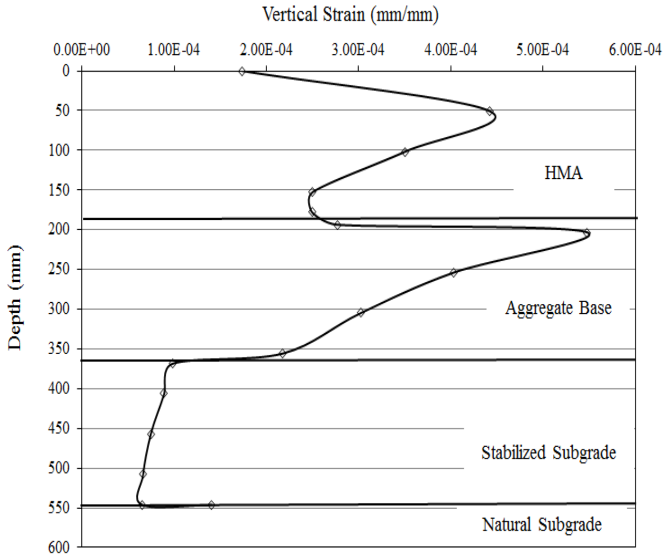

Fig. 5. Typical Vertical Strain Distributions in the Test Section (at the Center of a Wheel Load).

$$\varepsilon_t = C_3\left(\frac{1}{4}th\ tandem\ axle\ weight\right) + C_4 \quad (3)$$

where,
ε_t = Vertical strain from tandem axle, and
C_3, C_4 = Regression constants.

Step-3: In this step, vertical strains/kN for steering axles and tandem axles were calculated for that particular temperature. The vertical strain/kN from all the steering and tandem axles of different vehicles at that particular hour and temperature was calculated using Eqs. (4) and (5), as noted below:

$$\varepsilon_s = \frac{\varepsilon_{s1}+\varepsilon_{s2}+\varepsilon_{s3}+ \ldots\ldots\ldots\ldots + \varepsilon_{sn}}{W_{s1}+W_{s2}+W_{s3}+ \ldots\ldots\ldots\ldots + W_{sn}} \quad (4)$$

where,
ε_s = Vertical strain of steering axles /kN,
ε_{s1}, ε_{s2}, ε_{s3}, ε_{sn} = Vertical strains due to half- steering axles of Vehicle 1, Vehicle 2, Vehicle 3 and Vehicle n, respectively, and
W_{s1}, W_{s2}, W_{s3}, W_{sn} = Half-weight (kN) of steering axles of Vehicle 1, Vehicle 2, Vehicle 3 and Vehicle *n*, respectively.

$$\varepsilon_t = \frac{\varepsilon_{t11}+\varepsilon_{t12}+\varepsilon_{t13}+\varepsilon_{t14}+\varepsilon_{t21}+ \ldots\ldots\ldots\ldots + \varepsilon_{tnn}}{W_{t11}+W_{t12}+W_{t13}+W_{t14}+W_{t21} \ldots\ldots\ldots\ldots + W_{tnn}} \quad (5)$$

where,
ε_t = Vertical strain of tandem axles /kN, ε_{t11}, ε_{t12}, ε_{t13}, ε_{t14} = Vertical strains due to ¼ tandem axles of Vehicle 1,
ε_{t21} = Vertical strains due to ¼ of tandem axle 1 of Vehicle 2,
ε_{tnn} = Vertical strains due to ¼ tandem axle n of Vehicle *n*,
W_{t11}, W_{t12}, W_{t13}, W_{t14} = ¼ Weight (kN) of tandem axles of Vehicle 1,
W_{t21} = ¼ Weight (kN) of tandem axle 1 of Vehicle 2, and
W_{tnn} = ¼ Weight (kN) of tandem axle n of Vehicle *n*.

Step-4: WinJULEA simulations were conducted (following Step - 1 through Step - 3 several times) for a wide range of temperatures (from 10℃ to 43℃) that are representative of pavement temperatures in the Test Section, in order to obtain the vertical strain-temperature correlations. Two separate vertical strain-temperature correlations were obtained to predict vertical strain on the top of the aggregate base layer as a function of pavement temperature: one for steering axle and the other for tandem axle.

Following the steps described in Step-1 through Step-4, the final correlations between vertical strain on the top of the aggregate base layer and the mid-depth pavement temperature for single and tandem axles was established, as presented in Eqs. (6) and (7).

$$\varepsilon_s = 3 \times 10^{-07}\, T^{1.2127} \quad (R^2 = 0.99) \quad (6)$$

$$\varepsilon_t = 6 \times 10^{-07}\, T^{1.0682} \quad (R^2 = 0.99) \quad (7)$$

where,
ε_s = Vertical strain per kN per steering axle for a particular temperature,
ε_t = Vertical strain per kN per tandem axle for a particular temperature, and
T = Mid-depth pavement temperature (°C).

Traffic Data for Vertical Strain Calculation

As mentioned earlier, the vehicle category, axle weight, and loading configuration of each vehicle travelled over the Test Section was recorded at the WIM station. From May 30, 2008 to May 2, 2012, approximately a total of 4.5 million single axles and 14.2 million tandem axles have passed over the Test Section, with a total of 32,600 hours of vehicle data were collected at the WIM station within that timeframe. Since temperature was recorded every hour, vertical strains/kN from steering and tandem axles was calculated using Eqs. (6) and (7) for every hour. Then, average hourly vertical strains for both steering and tandem axles were calculated using Eqs. (8) and (9).

$$\varepsilon_{si} = \varepsilon_s\left(\frac{W_{s1}+W_{s2}+W_{s3}+ \ldots\ldots\ldots\ldots + W_{sn}}{N_{si}}\right) \quad (8)$$

$$\varepsilon_{ti} = \varepsilon_t\left(\frac{W_{t11}+W_{t12}+W_{t13}+W_{t14}+W_{t21} \ldots\ldots\ldots\ldots + W_{nn}}{N_{ti}}\right) \quad (9)$$

where,
ε_{si} = Average hourly vertical strain from steering axles,
ε_{ti} = Average hourly vertical strain from tandem axles,
N_{si} = Total number of steering axle passes at that particular hour, and
N_{ti} = Total number of tandem axle passes at that particular hour.

The traffic data were linked with the environmental database (temperature) with the assistance of a time stamp (i) and thereby at any given time, the vertical strain produced by a certain number of axle passes was available.

The VSB Rut Prediction Model

Rut measurements, made at approximately every three months, were linearly interpolated to have a rut value for each hour of each day. Since rut was measured at six stations, each trip's rut values were averaged to obtain one rut value for that particular field trip. By relating the measured hourly rutting to the vertical strain on the top of the aggregate base layer and the total number of steering and tandem axle passes, the rut prediction model was developed by performing a nonlinear regression analysis using the least–square technique in the Microsoft Excel spread sheet. The general form of the VSB rut prediction model is given in Eq. (10).

$$Rut_i = Rut_{i-1} + \lambda_1 (N_{si}^{\lambda_2 \varepsilon_{si}} + N_{ti}^{\lambda_3 \varepsilon_{ti}}) \tag{10}$$

where,
Rut_i = Rut at time "i" from field measurements,
Rut_{i-1} = Rut at time "i-1" from field measurements,
N_{si} = Total number of steering axle passes at time "i",
N_{ti} = Total number of tandem axle passes at time "i",
λ_1 = Regression constant for traffic (both steering and tandem axles), and
λ_2, λ_3 = Regression constants for vertical strain.

The final form of the VSB rut prediction model is given in Eq. (11).

$$Rut_i = Rut_{i-1} + 8.85\times10^{-07}(N_{si}^{1.55\times10^2 \varepsilon_{si}} + N_{ti}^{4.38\times10^2 \varepsilon_{ti}}) \quad (R^2 = 0.78) \tag{11}$$

When rut was predicted using the developed VSB model (Eq. (11)), the R^2 value, based on the predicted and the measured rut values, was found to be 0.78. A statistical method called 'student pair t-test' was conducted to compare the predicted and measured rut values using the VSB model. The null hypothesis for this analysis was that the difference in predicted and measured rut values was equal to zero and an alternative hypothesis was that rut values were not equal. The test was conducted at a significance Level of 0.05. The p-value of 0.05 or less indicates rejection of the null hypothesis. The p-value for measured and predicted rut using the VSB model was found to be 0.18, which is significantly higher than 0.05 ($p>0.05$), indicating that no statistical difference exists between the measured and predicted rut. Further, the positive coefficients for both traffic and vertical strains show that an increase in the number of axle passes and strain levels will increase the rutting, as expected. Fig. 6 shows the predicted rutting from the VSB model and the measured average rutting of all stations, as a function of cumulative number of axles. Overall, the VSB model predicted the field rutting reasonably well.

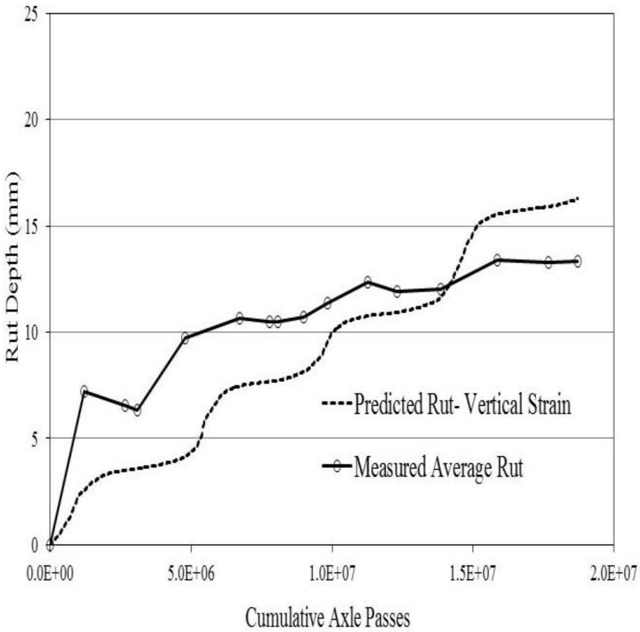

Fig. 6. Vertical Strain Model: Predicted and Measured Rut in the Test Section.

Shear Strain-based (SSB) Rut Prediction Model

As mentioned earlier, rut is considered to be a combination of two mechanisms. At the beginning, rut is generally governed by the accumulation of vertical strain in the form of additional compaction, and afterwards rut is generally governed by the shear flow in the HMA layer. Also, several researchers [7, 9, 13] have shown that controlling only vertical strain on the top of roadbed soil does not efficiently control pavement rutting. Some studies also showed that vertical strain based approach works better in predicting base layer and subgrade layer rutting than HMA layer rutting. Therefore, a separate rut prediction model, based on the shear strain in the HMA layer, was developed. The methodology used to develop the SSB rut prediction model was similar to the methodology used to develop the VSB model. The only difference was that the vertical strain was substituted by the maximum shear strain.

Maximum Shear Strain Computation

The approach to compute shear strain was similar to the approach used for computing vertical strain. However, the shear strain was computed at different depths in the HMA layer using WinJULEA. A similar approach was used by Selvaraj [9] for developing rut prediction model from the HMA layer. Depending upon the vehicle weight, the maximum shear strain was observed at the tire's edge and at a depth of about 12.7-mm to 51-mm below the pavement surface. A typical shear strain profile at different depths and at different distances from the center of a tire load is presented in Fig. 7. It is observed that the maximum shear strain for a particular load is located at the tire's edge (66-mm). The dotted line in Fig. 7 represents the maximum shear strain profile in the HMA layer. It is also observed from Fig. 7 that at a depth of approximately 30.5-mm from the surface, the shear strain value reaches its maximum and after that the shear strain value starts to decrease. A recent study by Yoo and Al-Qadi [15] also showed that the maximum shear strain was found at a depth of about 25.4-mm from the pavement surface.

Shear Strain-Temperature Correlations Development

An approach similar to that adopted for developing vertical strain-temperature correlations was followed for developing the shear strain-temperature correlations. The only difference is that the vertical strain was replaced by shear strain in Step-2 to Step-4 discussed earlier in the "Vertical Strain-Temperature Correlations" section. Also, in the case of shear strains, steering and tandem axles were analysed separately. The final shear strain-temperature correlation for single axle and tandem axles are presented in Eqs.

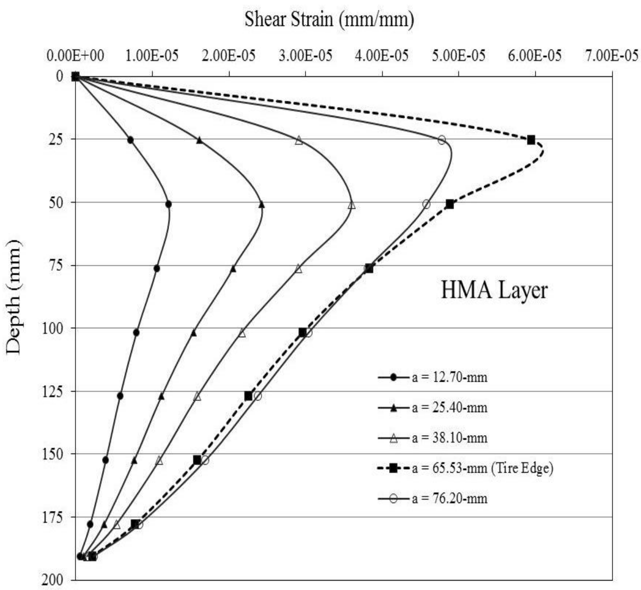

Fig. 7. Typical Shear Strain Distribution in the HMA Layer of the Test Section(a = Distance from the Center of a Wheel Load).

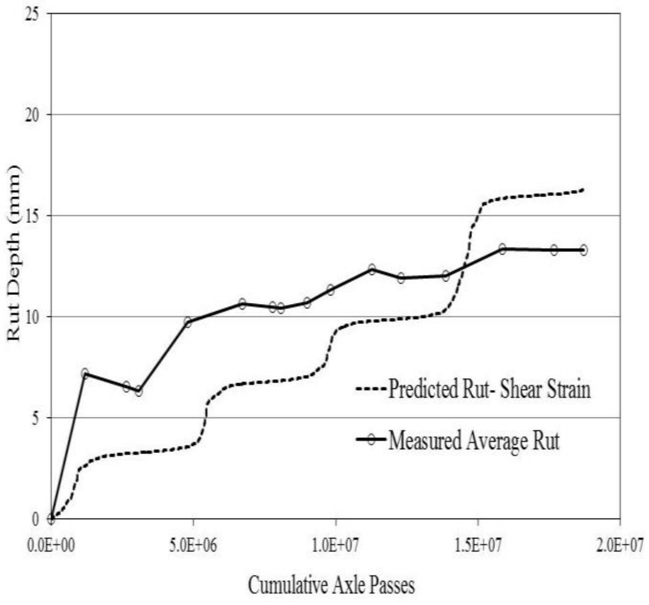

Fig. 8. Shear Strain Model: Predicted and Measured Rut in the Test Section.

(12) and (13).

$$\gamma_s = 3 \times 10^{-7}\, T^{1.2189} \quad (R^2 = 0.98) \tag{12}$$

$$\gamma_t = 7 \times 10^{-7}\, T^{0.9548} \quad (R^2 = 0.98) \tag{13}$$

where,
γ_s = Maximum shear strain per kN per steering axle for a particular temperature,
γ_t = Maximum shear strain per kN per tandem axle for a particular temperature, and
T = Mid-depth pavement temperature (°C).

The SSB Rut Prediction Model

The procedure for collecting traffic data for shear strain calculation was similar to that described in case of vertical strain. The same approach described for the VSB model building was used to develop the SSB model. The final form of the SSB rut prediction model is presented in Eq. (14).

$$Rut_i = Rut_{i-1} + 8.85\times10^{-07}(N_{si}^{9.20\times10^2\gamma_{si}} + N_{ti}^{2.93\times10^2\gamma_{ti}}) \quad (R^2 = 0.72) \tag{14}$$

where,
γ_{si} = Average hourly shear strain from steering axles, and
γ_{ti} = Average hourly shear strain from tandem axles.

When rut was predicted using the developed SSB model (Eq. (14)), the R^2 value, based on the predicted and measured rut values, was found to be 0.72. Student's t-test conducted on the measured and predicted rut using the SSB model generated a p-value of 0.16 ($p > 0.05$) which indicates that no statistical difference exists between the measured and predicted rut using the SSB model. Furthermore, the positive coefficients for both traffic and shear strains indicate that an increase in number of axle passes and strain levels will increase the rutting, as expected. Fig. 8 shows the predicted rutting from the SSB model and the measured average rutting of all stations from the Test Section, as a function of cumulative number of axles. Overall, the SSB model also predicted the field rutting reasonably well.

Comparison of VSB and SSB Based Rut Models

As both models predicted field rut reasonably well, an attempt was made to compare the two models. Table 1 shows a comparison between the two models. Rut measurements from the field were taken as a reference to compare rut prediction efficiency of the two models. From Table 1, it is evident that, although in 14 occasions out of 15, the SSB model has higher percentage differences from the field rut measurements than the VSB model, the differences are not very significant. A statistical analysis, called student's pair t-test, was performed at a significant level (p=0.05) to verify the performance of both the models (VSB and SSB). It was observed that the two-tail p-values for the two models were 0.20 ($p > 0.05$), indicating that no statistically significant difference exists between the two models.

Similar rut prediction models were developed from the NCAT test track by Selvaraj [9]. According to Selvaraj [9], both the VSB and SSB model accurately predicted rutting on a section-by-section basis, but the SSB model outperformed VSB model when sections were grouped according to binder modification. However, in the present study, both VSB and SSB models were observed to perform with similar level of accuracy.

Conclusions

From approximately four years of pavement, traffic, and environmental data, two rut prediction models were developed. Actual vehicular traffic and environmental data from an in-service pavement was used to develop the models. The WinJULEA was

Table 1. Comparison of Vertical and Shear Strain-based Models.

Date	Measured Average Rut Depth (mm)	VSB Model Predicted Rut Depth (mm)	Percent Difference (VSB Model)	SSB Model Predicted Rut Depth (mm)	Percent Difference (SSB Model)
August 21, 2008	7.20	2.71	62	2.99	59
December 3, 2008	6.56	3.75	43	3.62	45
January 8, 2009	6.35	3.84	40	3.67	42
May 19, 2009	9.72	4.41	55	3.97	59
October 28, 2009	10.65	7.98	25	7.41	30
February 16, 2010	10.49	8.20	22	7.53	28
March 10, 2010	10.47	8.26	21	7.56	28
May 18, 2010	10.69	8.67	19	7.78	27
August 11, 2010	11.35	10.17	10	9.58	16
November 22, 2010	12.36	11.47	7	10.82	12
February 14, 2011	11.94	11.66	2	10.93	8
June 7, 2011	12.04	12.40	3	11.41	5
October 18, 2011	13.38	16.59	24	17.67	32
February 22, 1012	13.28	16.97	28	17.88	35
May 2, 2012	13.33	17.37	30	18.10	36

used to develop correlations between temperature and strains induced from vehicular traffic. Various field tests including FWD tests and field rut measurements were performed periodically in this study. The following concluding remarks can be drawn based on the results presented in the preceding sections:

(1) Two significantly different methods, namely straight edge-rut gauge combination and Face Dipstick® were used to measure rut in the Test Section. It was observed that Face Dipstick® provided more consistent and accurate rut measurements than straight edge-rut gauge combination.

(2) Field rut measurements show that all stations in the I-35 Test Section have undergone both primary and secondary rutting. After about four years of service, no tertiary rut was observed at any station.

(3) Most of the rut was accumulated during the summer months. Although the cumulative number of axles during each summer month was similar, the rate of rutting was much higher in the first summer month than in the subsequent summer months.

(4) Both the VSB and SSB models predicted rut with similar level of accuracy, as evident from the high R2 values (0.78 for VSB and 0.72 for SSB model).

It should be noted that the field rut prediction models developed in this study were based upon moderate climatic conditions in Central Oklahoma. Also, the field rut prediction models are primarily applicable for similar pavement cross sections. Therefore, validation of the models is recommended for regions where pavement temperatures often go below -7℃ and for high temperature regions where pavement temperatures often go above 47℃ and also for different pavement cross sections. Since the Test Section is on I-35, and has extremely high traffic volume, it was not practical to close the lanes frequently to collect rut data. The rut prediction models developed in this study could be improved by including additional field rut data.

Acknowledgements

The authors wish to express their appreciation to Ginger McGovern, David Streb, Jeff Dean, Bryan Hurst, and Chris Westland from ODOT for their direct and indirect assistance with this research. Many others from ODOT made valuable contribution to this project. Bryan Cooper from ODOT deserves special thanks for his considerable effort and contributions in the construction and instrumentation phase of this project. Assistance of Marc Breidy, a former graduate student of CEES, is greatly appreciated. The authors are thankful to colleagues at the NCAT for their assistance with the instrumentation of the test section. Special thanks are due to Dr. David Timm and Angela Priest.

References

1. AASHTO (2004). Guide for Mechanistic-Empirical Design of New and Rehabilitated Pavement Structures. Final Report prepared for National Cooperative Highway Research Program (NCHRP), Transportation Research Board, National Research Council, Washington, DC, USA.
2. Allen, D. and Deen, R.C. (1980). Rutting Models for Asphaltic Concrete and Dense Graded Aggregate from Repeated Load Tests. *Proceedings of the Association of Asphalt Paving Technologists*, Vol. 1, pp. 653-667.
3. Leahy, R.B. (1989). Permanent Deformation Characteristics of Asphalt Concrete. Ph.D. Dissertation. University of Maryland, College Park, Maryland, USA.
4. Williams, R.C., Hill, D.W., and Rottermond, M.P. (2005). Utilization of an Asphalt Pavement Analyzer for Hot Mix Asphalt Laboratory Mix Design. *Journal of ASTM International*, 2(4), pp. 16-40.
5. Ali, H.A., Tayabji, S.D., and Torre, F.L. (1998). Calibration of Mechanistic-Empirical Rutting Model for In-Service Pavements. *Transportation Research Record*, 1629, pp. 159-168.
6. Hand, A.J., Epps, J.A., and Sebaaly, P.E. (1999). Development of APT Based Permanent Deformation Prediction Models Translatable to Other Environments. *Accelerated Pavement Testing International Conference*, Reno, Nevada, USA.
7. Kim, H.B., Buch, N., and Park, D.Y. (2000).

Mechanistic-Empirical Rut Prediction Model for In-Service Pavements. *Transportation Research Record*, 1730, pp. 99-109.
8. Zhou, F., Scullion, T., and Sun, L. (2004). Verification and Modeling of Three-Stage Permanent Deformation Behavior of Asphalt Mixes. *Journal of Transportation Engineering*, ASCE, 130(4), pp. 486-494.
9. Selvaraj, S.I. (2007). Development of Flexible Pavement Rut Prediction Models from the NCAT Test Track Structural Study Sections Data. Ph.D. Dissertation, Auburn University, Auburn, Alabama, USA.
10. Hossain, N. (2010). Observed and Predicted Rut Behaviour of an Instrumented Test Section on I-35. M.S. Thesis, The University of Oklahoma, Norman, Oklahoma, USA.
11. Highway Research Board (HRB) (1962). The AASHO Road Test, Report 5 [online]. Available from: http://www.highways.gov.sk.ca/docs/reports_manuals/manuals/STP_DOC/stp240-20.pdf. Accessed August 11, 2010.
12. Finn, F., Saraf, C., Kulkarni, R., Nair, K., Smith, W., and Abdullah, A. (1977). The Use of Distress Prediction Subsystems for the Design of Pavement Structures. *Proceedings of the Fourth International Conference on the Structural Design of Asphalt Pavements*, Ann Arbor, Michigan, USA, pp. 3-37.
13. Theyse, H L., De Beer, M., and Rust, F.C. (1996). Overview of South African Mechanistic Pavement Design Method. *Transportation Research Record*, 1539, pp. 6-17.
14. Monismith, C.L. (1992). Analytically Based Asphalt Pavement Design and Rehabilitation: Theory to Practice. *Transportation Research Record*, 1354, pp. 5-26.
15. Yoo, P.J. and Al-Qadi, I.L. (2007). Effect of Transient Dynamic Loading on Flexible Pavements, *Transportation Research Record*, No. 1990, pp. 129-140.